ANL/CMT/CP-99407

THE BEHAVIOR OF SILICON AND BORON IN THE SURFACE OF CORRODED NUCLEAR WASTE GLASSES: AN EFTEM STUDY

E. C. Buck*, K. L. Smith**, and M. G. Blackford**
*Argonne National Laboratory
**Australian Nuclear Science and Technology Organization

ABSTRACT

Using electron energy-loss filtered transmission electron microscopy (EFTEM), we have observed the formation of silicon-rich zones on the corroded surface of a West Valley (WV6) glass. This layer is approximately 100-200 nm thick and is directly underneath a precipitated smectite clay layer. Under conventional (C)TEM illumination, this layer is invisible; indeed, more commonly used analytical techniques, such as x-ray energy dispersive spectroscopy (EDS), have failed to describe fully the localized changes in the boron and silicon contents across this region. Similar silicon-rich and boron-depleted zones were not found on corroded Savannah River Laboratory (SRL) borosilicate glasses, including SRL-EA and SRL-51, although they possessed similar-looking clay layers. This study demonstrates a new tool for examining the corroded surfaces of materials.

INTRODUCTION

Following the initial high dissolution rate of waste glasses (forward rate), there is a significant drop in the dissolution rate as the reaction progresses. This behavior is interpreted and modeled by assuming silicic acid (H_4SiO_4) saturation with respect to the dissolving solid, an affinity reaction term [1]. However, Bourcier [2] has shown that regression analysis of release rate data cannot discriminate between either the Grambow reaction affinity model or a surface transportation model (i.e., diffusion term). Gin et al. [3] maintain that a "gel" layer forms on the corroded glass surface, and this layer acts as a diffusion barrier to the continued dissolution of the glass. Until now the direct evidence for "gel" layers has remained elusive. In this study, we present direct evidence of a silica-rich layer with (EFTEM), which may be the "gel" described by others [3]; however, this layer has only been found in a limited set of simulant waste glasses.

Reacted borosilicate glasses commonly exhibit a thin smectite clay layer that is clearly discernible by conventional transmission electron microscopy (CTEM). At the stage of glass reaction when the dissolution rate starts to drop, this layer is typically between 50 and 200 nm thick and consists of fine bundles of smectite clays oriented perpendicular to the surface. This layer is probably too porous to act as a diffusion barrier (see Figure 1).

Electron Energy-Loss Spectroscopy (EELS) is a well-established TEM technique that is based on the fact that the energy electrons lose as they pass through TEM specimens is determined by the crystal chemistry of the specimen (see Figure 2). Energy filtered imaging (EFI or EFTEM) is a relatively new technique wherein images and compositional maps of TEM specimens are formed using electrons from a limited sections of full EELS spectra [4]. Energy filtered imaging is quantitative, which means that the contrast seen in the images is directly related to the number of atoms per unit area [4]. Furthermore, the spatial resolution is better than that obtained with EDS [5] or secondary ion mass spectrometry [6], two techniques that have previously been used to profile elements through surfaces. Using EFI, we were able to directly observe the distribution of the major glass components, Si, B, and O, in various glasses. In some borosilicate glasses, direct evidence was found of a silica-rich layer, which may be a diffusion barrier.

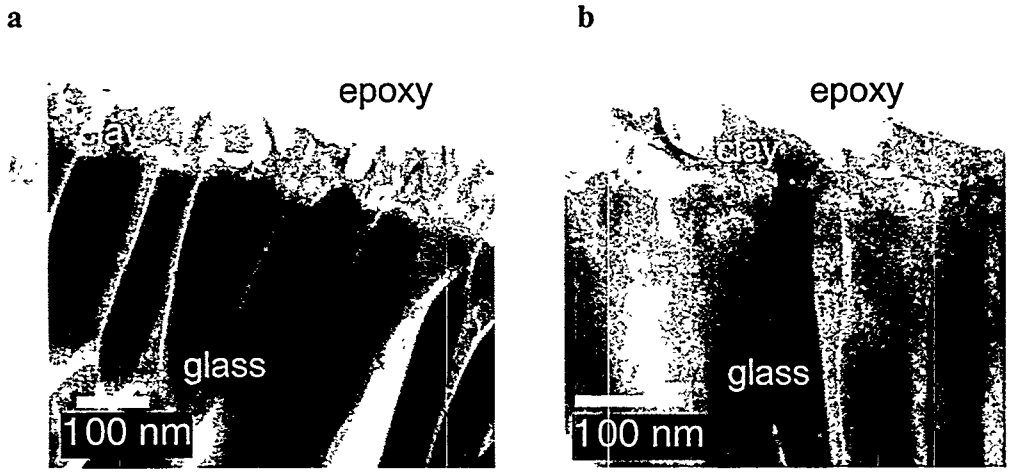

Figure 1. Thin clay layer visible from bright field TEM images of cross-sectioned (**a**) WV6 and (**b**) SRL-51S borosilicate glasses after 182 d reaction. With CTEM imaging the most prominent feature on the corroded surface was the smectite clay layer. The glass underneath displayed almost uniform contrast, indicating no compositional or structural changes. The samples were prepared by embedding corroded glass in epoxy and thin sectioning with an ultramicrotome. The glass shatters during this process, producing shards of glass which can be seen in the images.

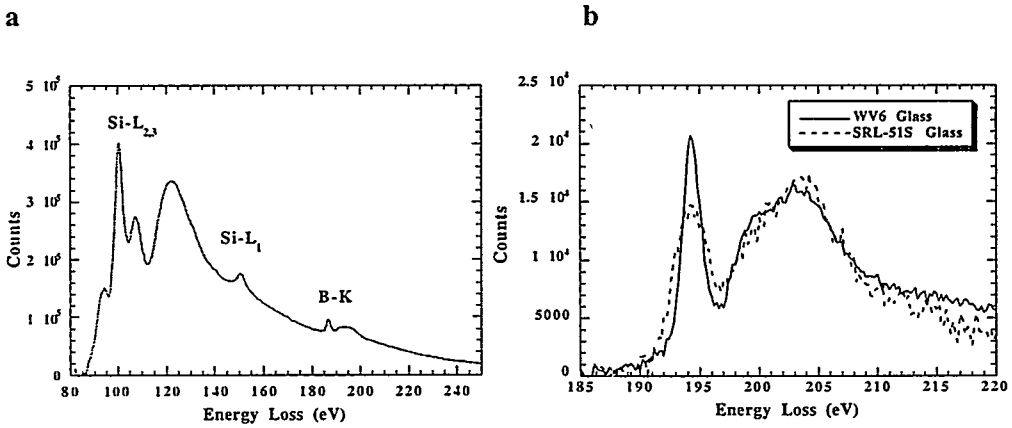

Figure 2. (**a**) Electron energy-loss spectroscopy of WV6 glass showing Si-$L_{2,3}$ and B-K edges. The B-K-edges for (**b**) WV6 glass and SRL-51S glass indicate that the WV6 glass has a higher level of trigonal boron compared to the SRL-51S glass.

EXPERIMENTAL PROCEDURE

We examined TEM specimens of two borosilicate glasses after they had been corrosion tested for various times. The glasses were a non-radioactive West Valley glass (WV6) and simulated SRL Tank 51 glass (SRL-51S) that were prepared at Argonne National Laboratory (ANL) and the Catholic University of America, respectively. The nominal compositions of the glasses are listed in Tables 1 and 2. These glasses are part of a suite of nuclear waste glasses that were reacted under extended Product Consistency Test-B (PCT-B) conditions [7] as follows. The glass was crushed and sieved into ~75-150 μm particles, then equal masses of sieved glass and EJ-13 simulated groundwater were placed in stainless steel Parr™ vessels. The initial glass surface area to leachant volume (S/V) ratio was 20,000 m^{-1}. Tests were maintained at 90°C for periods of 14 to 364 d. The solution analyses from these tests have been published in detail elsewhere [7].

DISCLAIMER

After the corrosion tests were terminated, selected particles of the reacted glass were extracted, embedded in an epoxy resin, and thin-sectioned with an ultramicrotome. The thin-sections were examined at the JEOL2010F-GIF2000 facility of the Australian Nuclear Science and Technology Organisation (ANSTO) and at the JEOL2000FXII-GIF200 facility of ANL.

Compositional maps were calculated using the "3-window method" [4]. Two pre-edge images were used to model and strip the background from under the post-edge region. Images were produced from the Si-$L_{2,3}$, B-K, and O-K edges. The EFTEM images were obtained at a microscope magnification of 1200x using 0.1 eV/channel dispersion, 2x binning, and exposure times ranging from 1 s to 10 s. The boron near edge structure describes the proportion of trigonal ($^{[3]}$B) and tetrahedral ($^{[4]}$B) boron in the glass [8,9].

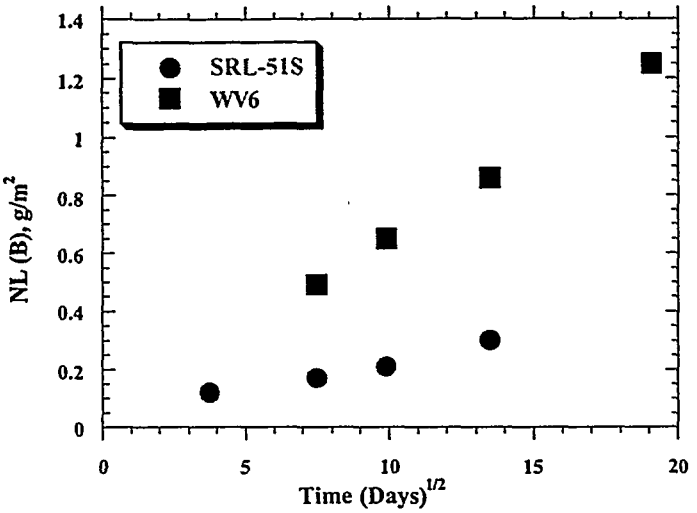

Figure 3. Plot showing release of boron from SRl-51S and WV6 glasses at an S/V of 20 000m^{-1} at 90°C versus root time. Adapted from Bates et al. [7]].

RESULTS

Corrosion Testing Results

As stated above, detailed solution analyses from all the corrosion tests that were conducted on the glasses in this study are published elsewhere [7]. Pertinent to this study is the fact that the reported release rates of boron from the WV6 glass are higher than those from the SRL-51S glass (see Figure 3). For example, after 182 d the release rates of boron from the SRL-51S and WV6 glasses were 0.3 and 0.85 g/m^2 respectively, whereas the measured Si concentrations, were 398 and 110 mg/L, and the pHs were 11.4 and 9.

Electron Energy-Loss Spectroscopy and Energy Filtered Imaging Results

The B-K core-loss edge can be used to probe the chemistry around B, providing information on the coordination environment and on the relative amounts of trigonal ($^{[3]}$B) and tetrahedral ($^{[4]}$B) boron in a sample [8,9]. The boron edge is characterized by two strong features; a sharp peak at ~194 eV (the edge feature of $^{[3]}$B) and the broader peak at 198-200 eV (the edge feature of $^{[4]}$B). The spectrum in Fig. 2b suggests that the WV6 glass possesses a higher level of $^{[3]}$B than SRL-51S, based on the relative intensities of these features.

Energy filtered imaging revealed the presence of silicon-rich zones on the corroded surface of WV6-45 glass directly underneath layers of precipitated smectite clay. The thickness of the silicon-rich layer on samples reacted at 20 000 m^{-1} varies from ~100 nm after 182 d to 200 nm thick after 364 d. Figure 4 shows EFTEM maps from a WV6 sample reacted at 20 000 m^{-1} for 182 d.

An extremely thin zone enriched in silicon was also seen on a WV6 glass specimen that had been reacted under less vigorous conditions (2 000 m^{-1}) for 30 days. Conventional TEM showed that the clay layer on this latter specimen was <10 nm thick and patchy and EFI silicon maps showed silicon enrichment to a depth of ~10 nm. These silicon-rich zones in all the specimens examined were not readily identifiable using EDS. Energy filtered mapping of the SRL-51S glass

reacted at 20 000 m^{-1} for 182 d (see Figure 5) shows no surface enrichment of silicon even though the clay layer has a similar thickness to the clay layer observed on the WV6 glass. The boron map showed the absence of boron in the clay layer.

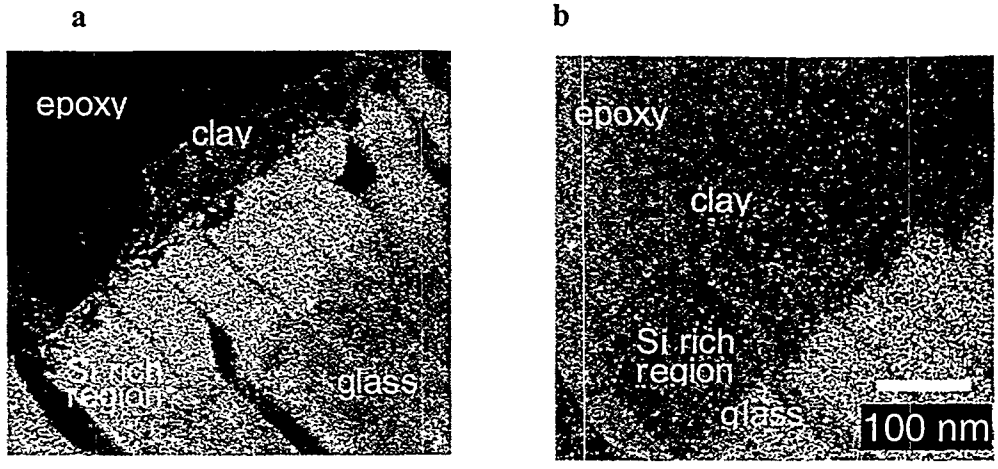

Figure 4. West Valley (WV6) glass reacted at 20 000 m^{-1} for 182 d. The oxygen map showed both the glass and the thin clay layer. The silicon map (**a**) showed the presence of an enriched region just underneath the clay layer. The boron map (**b**) revealed the complete absence of boron in the 150 nm thick layer underneath the clay layer.

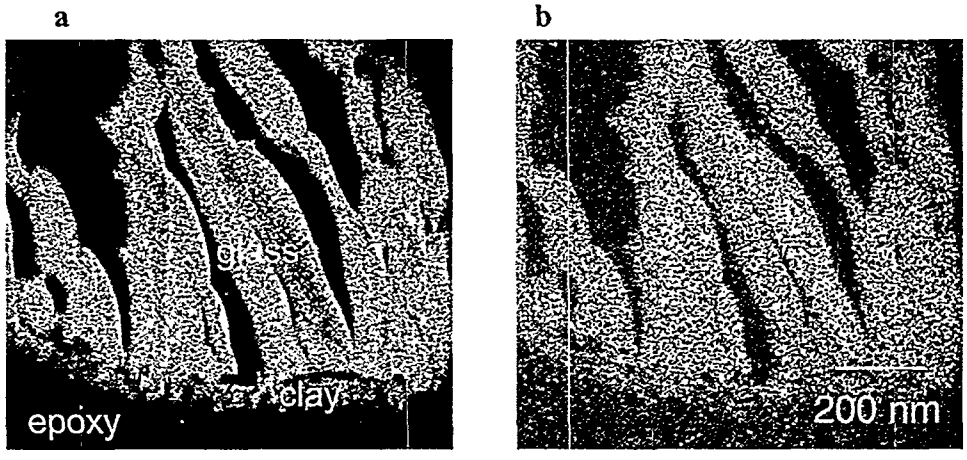

Figure 5. Savannah River Laboratory (SRL) Tank 51S simulated sludge glass reacted at 20 000 m^{-1} for 182 d. The silicon map (**a**) showed no enrichment of silicon even though the clay layer is similar in thickness to the layer observed in Figure 4. The boron map (**b**) indicated the absence of boron in the clay layer.

Table 1. Analyses[1] of WV6 Glass Reacted at an S/V of 20 000 m^{-1} for 182 d (n= number of measurements, s =standard deviation).

Oxide (wt%)	Clay Layer[2] (n=5)		Altered Si-Rich Region[2] (n=5)		Unreacted Glass[2] (n=5)		Reported Glass Composition[3,4]
	mean	s	mean	s	mean	s	
Na_2O[5]	2.38	0.34	0.55	0.16	0.43	0.44	10.42
MgO	4.68	0.18	0.37	0.10	0.75	0.17	1.16
Al_2O_3	13.79	0.63	10.86	0.32	9.55	0.26	7.82
SiO_2	51.86	0.94	61.14	2.51	63.20	1.75	53.43
P_2O_5	0.80	0.64	3.73	1.16	3.33	0.61	ND[6]
SO_3	0.74	0.24	0.43	0.05	0.39	0.13	ND[6]
K_2O	1.44	0.23	0.75	0.33	0.66	0.55	6.52
CaO	0.79	0.32	0.60	0.19	0.52	0.14	0.63
TiO_2	0.76	0.06	1.23	0.09	1.23	0.07	1.04
MnO	5.01	0.12	0.35	0.09	0.78	0.15	1.30
Fe_2O_3	13.45	0.23	12.22	0.39	12.03	0.86	15.64
NiO	0.21	0.07	ND[6]	–	ND[6]	–	0.33
ZrO_2	0.84	0.20	1.87	0.27	1.74	0.30	1.72
ThO_2	1.63	0.43	5.32	0.34	4.62	0.23	ND[6]
UO_2	ND	–	0.58	0.30	0.78	0.28	0.77
Total	98.40	–	100	–	100.00	–	100.00

Table 2. Analyses[1] of SRL51S Glass Reacted at an S/V of 20 000 m^{-1} for 182 d.

Oxide (wt%)	Clay Layer[2] (n=2)		Unreacted Glass[2] (n=6)		Reported Glass Composition[4]
	mean	s	mean	s	
Na_2O[5]	3.06	1.16	0.59	0.54	10.44
MgO	3.92	0.64	2.17	0.16	2.23
Al_2O_3	7.88	0.43	6.98	0.24	5.67
SiO_2	56.75	0.18	69.06	1.40	61.20
P_2O_5	1.36	0.19	1.14	0.10	0.61
SO_3	0.76	0.08	0.11	0.06	ND[6]
K_2O	0.44	0.27	0.33	0.31	1.51
CaO	0.39	0.16	1.54	0.17	1.51
Cr_2O_3	0.58	0.18	0.59	0.05	0.48
MnO	1.97	0.28	1.32	0.09	1.54
Fe_2O_3	18.94	0.79	14.48	0.34	13.32
NiO	0.57	0.13	0.37	0.04	0.30
UO_2	0.74	0.40	1.24	0.29	1.19
Total	97.32	–	99.90	–	100

[1] Data are normalized and exclude the major elements B and Li, as well as the minor elements, including rare earths and noble metals.

[2]Quantification performed with NIST DTSA software [see G. R. Lumpkin, K. L. Smith, and R. Gieré, *Micron* **28** (1994) 57-68]. Errors were 5% for most elements.

[3]W. L. Ebert, *Ceramic Trans.* **61** (1996) pg. 473.

[4]Dissolved and analyzed glass by mass spectrometry [6]. Reported uncertainty in measurement was approximately 15% for most elements.

[5]The focused electron probes in scanning and transmission electron microscopes cause alkali (in particular Na^+) migration in alkali aluminosilicate glasses and minerals, making chemical analyses of these phases difficult [see G. B. Morgan and D. London, *Amer. Mineral.* **81** (1996) 1176-1185].

[6]ND = no data available for this element.

DISCUSSION

The clays from the tests of WV6 and SRL-51S were enriched in Mg, Mn, and Ni relative to the glass and depleted in U (see Tables 1 and 2). These analyses of clay agree with previous tests with similar borosilicate glasses [5,6,10]. There was significant enrichment of Th, Zr, and P in the Si-rich layer in the WV6 glass.

The compositional variations in the WV6 and SRL-51S glass may account for the variation in boron coordination. The energetics of the charge balance mechanisms in borosilicate glass dictate that $NaAl^{3+}$ should form before $NaFe^{3+}$ or NaB^{3+}; Na is used to charge balance Al^{3+} and once all the Al is accounted for, NaB^{3+} will start to emerge [11]. This might explain the higher level of $^{[3]}B$ in the WV6 glass.

Although the WV6 boron release data (see Figure 3) follow a $t^{1/2}$ relationship, this does not prove that the observed Si-rich layer is a diffusion barrier. However, supporting evidence comes from EFTEM images obtained at 364 d where a 100-200 nm thick Si-enriched layer was also found. The SRL-51S boron release data do not appear to follow the $t^{1/2}$ relationship, and no Si-rich layer was observed with EFI. As the compositional maps represent concentrations [4], the Si-rich layer on the corroded WV6 glass has a higher concentration of silicon than the underlying uncorroded glass. This suggests that restructuring of the glass occurred as boron was leached from the surface. Changes in the deformation produced by the microtome in this region observed in some CTEM images also suggest restructuring of the glass. The Si-rich layer found in the corroded WV6 glass does agree with the models of glass corrosion presented by others [3] and, therefore, this layer might be the elusive "gel' layer.

CONCLUSION

We have a) demonstrated differences in B coordination between two types of borosilicate glass, b) proven the occurrence of Si-rich zones in corroded WV6 glass, c) shown that the level of boron within the Si-rich layer is low, and d) shown that the boundary between the Si-layer and glass underneath is very sharp. This study demonstrates that EELS and EFTEM are a powerful tools for characterizing and assessing the corrosion behavior of materials.

ACKNOWLEDGEMENTS

Tests were run by W. L. Ebert, J. K. Bates, and J. E. Emery. One of us (ECB) would like to thank the Australian Nuclear Science and Technology Organisation for providing financial support for a visit to their JEOL2010F-GIF2000 Microscopy Facility in Sydney, Australia.

REFERENCES

[1] D. M. Strachan, W. L. Bourcier, and B. P. McGrail, *Rad. Waste Mgmt. Environ. Res.* **19** (1994) 129-145.

[2] W. L. Bourcier, *Mater. Res. Soc. Symp. Proc.* **333** (1994) 69-82.

[3] S. Gin, E. Vernaz, C. Jégou, and F. Larche, Proc. 18th Inter. Congress on Glass (1998), Section **B10** pp. 64-69; G. Berger, C. Claparols, C. Guy, and V. Daux, *Geochim. Cosmo. Acta.* **58** (1994)4875-4886.

[4] F. Hofer, W. Grogger, G. Kothleitner, and P. Warbichler, *Ultramicroscopy*, **67** (1997) 83-103.

[5] J. K. Bates, D. L. Lam, and M. J. Steindler, *Mater. Res. Soc. Symp. Proc.* **15** (1983) 183-190.

[6] B. W. Biwer, J. K. Bates, T. A. Abrajano, and J. P. Bradley, *Mater. Res. Soc. Symp. Proc.* **176** (1990) 255-263

[7] J. K. Bates et al., ANL Technical Support Program for DOE Office of Environmental Management, Annual Report October 1994- September 1995 ANL-96/11 (1996).

[8] L. A. J. Garvie, P. R. Buseck, and A. J. Craven, *Amer. Miner.* **80** (1995) 1132-1144.

[9] M. E. Fleet and S. Muthupari, *J. Non Cryst. Sol.* **255** (1999) 233-241.

[10] W. L. Ebert, J. K. Bates, and W. L. Bourcier, *Waste Mgmt.* **11** (1994) 205-221.

[11] J. J. De Yoreo and A. Vanrotsky, *J. Am. Ceram. Soc.* **73** (1990) 2068-2072.